TGA Report

Nr. 8
Veröffentlicht: 03/2022
Bestell-Nr.: 403

Measurements of Aerosol Transfer by Rotary Heat Exchangers

Prof. Heinrich Huber, Hochschule Luzern – Technik & Architektur
Dipl.-Ing. HLKS Florian Brzezinski, Hochschule Luzern – Technik & Architektur
Dr. sc. nat. Michael Riediker, Swiss Centre for Occupational and Environmental Health

Report HP-212193 der Hochschule Luzern

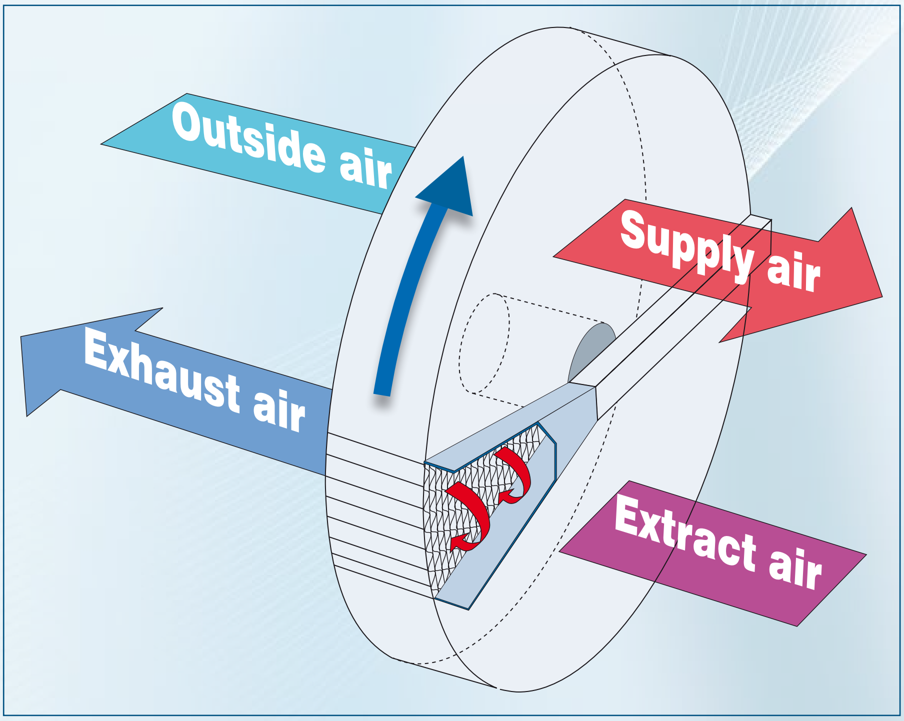

HSLU Hochschule Luzern

Fachverband Gebäude-Klima e.V.

Diese Studie entstand mit freundlicher Unterstützung folgender Unternehmen:

Hoval Aktiengesellschaft
Klingenburg GmbH
Swegon Group AB
Systemair GmbH
TROX GmbH

Fachverband Gebäude-Klima e.V.

Bewertung der Studie durch den Fachverband Gebäude-Klima e. V.

Die Covid-19-Pandemie beschäftigt uns nun schon seit etwa zwei Jahren. Dabei ist das Einatmen infektiöser Aerosole einer der Hauptübertragungswege. Mikrotröpfchen und Aerosole, die beim Atmen oder Sprechen in die Umgebungsluft gelangen, können hier über einen Zeitraum von mehreren Stunden verweilen und aktive Sars-CoV-2-Viren transportieren.

Grundlage der hier vorgestellten Studie ist die Fragestellung, inwieweit potenziell kontaminierte Aerosole durch Rotationswärmeübertrager von der Abluft in die Zuluft gelangen können. Mögliche Übertragungswege sind hier Leckagen, Mitrotation oder über das Material der Speichermasse. Also im Zusammenhang mit den Rotationswärmeübertragern die Frage, ob zusätzlich zu den bekannten Aspekten der Leckagen (allgemein in RLT-Geräten) weitere Übertragungswege und Risiken bestehen. Hierzu wurden Untersuchungen zur Aerosolübertragung auf einem Prüfstand des HLK-Labors der Hochschule Luzern durchgeführt.

Mögliche Leckagen bei der Verwendung von Rotationswärmeübertragern können durch korrekte Ventilatoranordnung und Druckverhältnisse, sowie durch Spülzonen minimiert bzw. so gerichtet werden, dass eine Übertragung von der Abluft auf die Zuluft praktisch ausgeschlossen wird. Die Oberfläche eines Rotationswärmeübertragers wird sowohl von der Zu- als auch von der Abluft berührt. Dies ermöglicht die Feuchterückgewinnung, könnte aber auch das Übertragen unerwünschter Stoffe bedingen.

Zur Beurteilung der Aerosolübertragung wurden das Abluftübertragungsverhältnis EATR (Maß für die Übertragung gasförmiger Stoffe von der Abluft auf die Zuluft) und das Aerosolübertragungsverhältnis ASTR (Maß für die entsprechende Aerosolübertragung) bestimmt und verglichen. Die Messungen wurden mit zwei handelsüblichen Rotationswärmeübertragern verschiedener Hersteller (ein Kondensations- und ein Sorptionsrotor) sowohl für den Heiz- als auch für den Kühlfall und mit Feuchteübertragung durchgeführt. Für beide Komponenten wurden die Versuchsreihen sowohl mit als auch ohne Spülkammer durchgeführt. Die Anströmgeschwindigkeit der Rotationswärmeübertrager lag bei 2 m/s. Das für die Bestimmung des ASTR verwendete Aerosol ist mit jener vom Menschen ausgeatmeten Aerosole vergleichbar. Dieses Aerosol ist in der Luft über längere Zeiträume stabil. Die Erfassung des EATR erfolgte durch das Injizieren von Tracergas in die Abluft des Wärmerückgewinnerprüfstandes.

Bei allen betrachteten Temperatur- und Feuchtebedingungen lagen die Werte für das Aerosolübertragungsverhältnis ASTR ohne Spülzone unter den Werten des Abluftübertragungsverhältnisses. Bei den Messungen mit Spülzone und sonst gleichen Bedingungen waren sowohl die EATR- als auch die ASTR-Werte stets sehr gering (ASTR und EATR maximal 0,6 %).

Zusammengefasst wurde festgestellt, dass neben einer möglichen Aerosolübertragung durch Leckagen bei Rotationswärmeübertragern kein zusätzliches Risiko der Aerosolübertragung über weitere Transportmechanismen besteht. Das ASTR ist mit den bekannten EATR-Kennwerten ausreichend genau abschätzbar.

Damit ist nachgewiesen, dass bei der fachgerechten Anwendung von Rotationswärmeübertragern unter Berücksichtigung der EATR-Kennwerte ein sicherer Betrieb von Lüftungsanlagen ohne erhöhtes Risiko der Aerosolübertragung möglich ist.

Comment to the study by Fachverband Gebäude-Klima e. V.

The Covid 19 pandemic kept us busy for about two years now. Inhalation of infectious aerosols is one of the main routes of transmission. Microdroplets and aerosols that enter the ambient air when breathing or talking can linger here for a period of several hours and transport active Sars-CoV-2 viruses.

The basis of the study presented here is the question of the extent to which potentially contaminated aerosols can pass from the extract air into the supply air through rotary heat exchangers. Possible transfer paths are leakage, carry over or given by the rotor material itself. Thus, in connection with rotary heat exchangers, the question arises as to whether, in addition to the known aspects of leakage (generally in air handling units), further transmission paths and risks exist. For this purpose, investigations on aerosol transmission were carried out on a test rig of the HVAC laboratory of the Lucerne University of Applied Sciences and Arts.

Possible leakages when using rotary heat exchangers can be minimized by correct fan arrangement and pressure ratios, as well as by purge zones, or directed in such a way that a transfer from the extract air to the supply air is practically excluded. The surface of a rotary heat exchanger is contacted by both supply and extract air. This allows moisture recovery, but could also condition the transfer of undesirable substances.

To evaluate aerosol transfer, the exhaust air transfer ratio EATR (a measure of the transfer of gaseous substances from the extract air to the supply air) and the aerosol transfer ratio ASTR (a parameter of the corresponding aerosol transfer) were determined and compared. The measurements were carried out with two commercially available rotary heat exchangers from different manufacturers (one condensing and one sorption rotor) both for heating and cooling and with moisture transfer. For both components, the test series were carried out both with and without a purge sector. The face velocity of the rotary heat exchangers was 2 m/s.

The aerosol used for the determination of the ASTR is comparable to the aerosol exhaled by humans. This aerosol is stable in the air over longer periods of time. The EATR was determined by injecting tracer gas into the extract air of the heat recovery test rig.

For all temperature and humidity conditions considered, the aerosol transfer ratio ASTR without purge zone were lower than the exhaust air transfer ratio. In the measurements with purge sector and otherwise the same conditions, both the EATR and ASTR values were always very low (ASTR and EATR maximum 0,6 %).

In summary, it was found that in addition to possible aerosol transfer through leakage in rotary heat exchangers, there is no additional risk of aerosol transfer via other transport mechanisms. The ASTR can be estimated with sufficient accuracy using the known EATR characteristics.

It has thus been demonstrated that safe operation of ventilation systems without increased risk of aerosol transfer is possible when rotary heat exchangers are used properly considering the EATR characteristic values.

Lucerne University of
Applied Sciences and Arts

HOCHSCHULE
LUZERN

Technik & Architektur

Report HP-212193

Horw, 2022-03-01

Measurements of Aerosol Transfer by Rotary Heat Exchangers

Commissioned by
Fachverband Gebäude-Klima e. V.

Imprint

Commissioned by
Fachverband Gebäude-Klima e. V.
Danziger Strasse 20
D-74321 Bietigheim-Bissingen
Deutschland
(Abbreviation: FGK)

Contractor
Hochschule Luzern – Technik & Architektur
Prüfstelle Gebäudetechnik
Technikumstrasse 21
CH-6048 Horw
Schweiz
(Abbreviation: HLSU)

Subcontractor
Swiss Centre for Occupational and Environmental Health
Binzhofstrasse 87
CH-8404 Winterthur
Schweiz
(Abbreviation: SCOEH)

Authors
Prof. Heinrich Huber, HSLU T&A
Dipl. Ing. HLKS Florian Brzezinski, HSLU T&A
Dr. sc. nat. Michael Riediker, SCOEH

Delivered to
Claus Händel, FGK

Project No
HP-212193

File name
r_20220301 HP-212193 FGK Aerosol Transfer Measruements.docx

List of amendments

Version	Date	Status	Amendments / Remarks	Visa
No 01	02.02.2022	V0	Draft Final Report	Brf, Huh
No 02	01.03.2022	V1	Final Report	Brf, Huh

Abstract

Since spring 2020, the Sars-CoV-2 virus has been spreading, leading to the COVID-19 pandemic. The main route of transmission has been identified as inhalation of virus-containing aerosols. The microdroplets released during breathing (diameter ranging from 0.2 to 2 µm) or speaking (bimodal, microdroplets between 0.1 to 10 µm, and larger droplets between 20 to 1000 µm) [3] can remain airborne for hours depending on environmental conditions (temperature, humidity, light) and transport active Sars-CoV-2 viruses. In this context, the question has arisen to what extent potentially contaminated aerosols can be transferred by rotary heat exchangers (RHE) from the exhaust air to the supply air. Possible transmission paths of aerosols in rotors are leakage, carry over and given by the rotor material itself. For to answer this question a project led by of the association FGK Fachverband Gebäude-Klima e. V. has been initiated.

Test objects were a commercial condensation rotor and a commercial sorption rotor. The test took place at the test rig of the HVAC laboratory of the Hochschule Luzern. The aerosol concentration was measured in all four air streams (outside air, supply air, extract air, exhaust air). To keep the aerosol concentration in the outside air as low as possible, it was passed through an H14 filter. In the exhaust air inlet, the aerosol feed was built up. During the measurement, the aerosol was applied using a pulse method. The maximum peak heights at the four aerosol measuring points were used for evaluation.
A mixture of triethylene glycol, monopropylene glycol and dipropylene glycol was used as the aerosol source. The aerosol used has an average diameter of just over one micrometer and is therefore comparable in size to exhaled aerosol. The aerosol, like human exhaled aerosol, is liquid at normal ambient temperatures. It is produced by evaporation and condensation of a water-glycol mixture and is stable in air for extended periods of time. Parallel to the aerosol transfer, the exhaust air transfer ratio (EATR) was determined with tracer gas. For the aerosol measurements and evaluations, the HSLU collaborated with the institute SCOEH.

For the condensation rotor and the sorption rotor without a purge sector, the aerosol transfer ratio (ASTR) was always lower than the EATR with the tracer gas SF_6. The smallest difference of 0.1 to 0.5 percentage points was found at the lowest tested outdoor air temperature of -3°C. At higher outdoor air temperatures, the ASTR was between 0.5 and 2 percentage points lower than the EATR. With purge sector and conditions (rotor speed, face velocity, pressure conditions) resulting in an EATR not higher than 0.03%, measurements on the sorption rotor showed a maximum ASTR of 0.12%. For the condensation rotor with a different purge sector design, the ASTR remained at a level of 0.17 to 0.35%. It is assumed that the difference lies in the fluidic phenomena of the purge sector and not in the matrix of the rotor.

Content

1. Introduction 5
2. Test object and Method 5
2.1. Test object 5
2.2. Test set-up 6
2.3. Test conditions and procedure 6
3. Results 7
3.1. Condensation Rotary Heat Exchanger without purge sector 7
3.2. Condensation Rotary Heat Exchanger with purge sector 9
3.3. Sorption Rotary Heat Exchanger without purge sector 11
3.4. Sorption Rotary Heat Exchanger with purge sector 13
4. Discussion 15
4.1. Significance of test conditions 15
4.2. Comparison of test results 15
4.3. Conclusion 18
5. List of Figures 19
6. Bibliography 19
7. Annex 2: Test Method 20
7.1. Aerosol Transfer Ratio ASTR 20
7.2. Exhaust Air Transfer Ratio EATR 21
7.3. Test Rig for Energy Recovery Devices 22
7.4. Symbols and Subscripts 23
8. Annex 2: Measurement Devices 24
8.1. Aerosol Generator/ Aerosol 24
8.2. Aerosol measuring device 24
8.3. Specification Instruments test rig for energy recovery devices 25

1. Introduction

Aerosols are considered a main cause of COVID-19 infections indoors, the disease caused by the virus SARS-CoV-2. Therefore, limiting aerosol transfer between supply and extract air in ventilation systems is critical. In bidirectional ventilation systems, heat recovery is state of the art and is even required in the European "Commission guidelines: Ecodesign required for ventilation units" (Regulation (EU) No 1253/2014). Rotary heat exchangers (RHE) are an efficient and economically interesting solution and are therefore widely used. A disadvantage of RHE is that due to the physical principle and the mechanical implementation a higher exhaust air transfer ratio (EATR) can occur than with other common heat recovery categories such as plate heat exchangers or run around coil systems. Measures to minimise and evaluate the EATR of RHEs are well known and recommended e.g. in the REHVA COVID-19 Guide [1]. Particular mention should be made here of the correct pressure ratios and purge sectors. However, RHEs are not generally equipped with purge sectors, and in older air handling units (AHUs) the pressure ratios are not always optimal. Another aspect is the fact that the surface of an RHE is touched by both supply and extract air. Although this enables humidity recovery, it also carries the risk of transferring undesirable substances. However, aerosols can adhere to the surface if they come into contact with it. Associated with adhesion are deposition and potential release.

The characteristics of RHEs raise the question of whether relevant aerosol transfer can take place and whether this differs from EATR. For hygienically demanding applications of RHEs, it is crucial to have more knowledge about the phenomenon of aerosol transfer. Additional knowledge is important for the acceptance of RHEs by both experts and occupants. Against this background, the industry is looking for answers. On the initiative of a private company, the University of Applied Sciences and Arts Lucerne (HSLU) together with the Swiss Centre for Occupational and Environmental Health (SCOEH) carried out first experimental investigations in January 2021. In autumn 2021, the idea to expand those experiments was supported by a manufacturer group under the lead of the association FGK Fachverband Gebäude-Klima e. V.. The present project was initiated by this group. In addition to the first project, investigations with different air conditions were of interest and also differences of aerosol transfer with and without purge sector.

2. Test object and Method

2.1. Test object

Test objects were two commercial rotary heat exchangers (RHE) from different manufactures. The test objects are specified in Table 1

Table 1: Test object specification

Type	Condensation Rotor	Sorption Rotor
Material and coating	Aluminium without coating	Aluminium zeolite coating
Free diameter	1220 mm	900 mm
Depth	200 mm	250 mm
Diameter of hub	130 mm	165 mm
Free face area	1.156 m^2	0.615 m^2
Purge system	yes [a]	yes [a]
Design rotor speed [b]	10 rpm	20 rpm

a The purge sector could be dismantled for certain test series.
b Rotor speed for which the purge sector is designed for

2.2. Test set-up

The Building Technology Laboratory of the HSLU operates a test rig for heat recovery components. In chapter *7 Annex 2: Test Method* the test schemes, symbols and definitions are shown. The RHEs were installed in a test casing of the laboratory. This corresponds to EN 380:2021 [2] test type A1.

The test equipment for aerosols was provided by SCOEH, which also supported the evaluation of the results. All other equipment and evaluations were provided by HSLU.

2.3. Test conditions and procedure

In order to assess the aerosol transmission, the exhaust air transfer ratio (EATR) and the aerosol transfer ratio (ASTR) were determined and compared.

The measurements of EATR and ASTR were performed with balanced air mass flows (exhaust inlet/supply outlet) under the conditions specified in Table 2 and Table 3. The thermal and fluidic quantities, as well as the EATR, were measured according to EN 380:2021 with precision class P1.

For both RHEs test series with and without purge sector were carried out.

Table 2: Measuring points assessed with condensation and sorption rotors

Meas.-points	Pressure difference SUP/ETA Cond./sorp. [a]	Face air velocity	Rotor speed Cond./sorp. [a]	Air inlet-temperatures		Air inlet Relative Humidity		Purge sector
	Δp_{22-11} Pa	c m/s	n rpm	t_{21} °C.	t_{11} °C.	φ_{21} % RH	φ_{11} % RH	
1	10/20	2.0	9/10	20.0	20.0	50	50	yes/no
2	10/20	2.0	10/15	20.0	20.0	50	50	yes/no
3	10/20	2.0	12/20	20.0	20.0	50	50	yes/no
4	10/20	2.0	9/10	2.0	22.0	70	45	yes/no
5	10/20	2.0	10/15	2.0	22.0	70	45	yes/no
6	10/20	2.0	12/20	2.0	22.0	70	45	yes/no
7	10/20	2.0	9/10	-3°	22.0	70	45	yes/no
8	10/20	2.0	10/15	-3°	22.0	70	45	yes/no
9	10/20	2.0	12/20	-3°	22.0	70	45	yes/no

a Values before slash for condensation rotor, after slash for sorption rotor

Table 3: Additional measuring points assessed with the sorption rotor

Meas.-points	Pressure difference SUP/ETA	Face air velocity	Rotor speed	Air inlet-temperatures		Air inlet Relative Humidity		Purge sector
	Δp_{22-11} Pa	c m/s	n rpm	t_{21} °C.	t_{11} °C.	φ_{21} % RH	φ_{11} % RH	
10	20	2.0	10	35.0	25.0	50	50	yes/no
11	20	2.0	15	35.0	25.0	50	50	yes/no
12	20	2.0	20	35.0	25.0	50	50	yes/no

3. Results

In the following the results of the tests are presented. For a description of the symbols and their definitions please refer to the appendix. The accuracy of the ASTR value is calculated from the standard deviation by multiplying by a coverage factor k (confidence level of 95%). The accuracy of the EATR is determined according to the ISO/IEC Standard Guide 98-3:2008 Typ B (confidence level of 95%).

3.1. Condensation Rotary Heat Exchanger without purge sector

Table 4: Aerosol Transfer Ratio (ASTR), Condensation Rotor, without purge sector

ASTR without purge sector	v m/s	t_{11} °C	φ_{11} % r.F.	t_{21} °C	φ_{21} % r.F.	p_{Baro} Pa	n rpm	q_{m22} kg/h	Δp_{22-11} Pa	ASTR %		Purge Sector
ASTR 1.1.1	2.0	19.8	50.6	20.7	47.8	95147	9.3	4987	10	1.47	± 0.12	no
ASTR 1.1.2	2.0	20.1	49.8	19.9	50.2	95099	10.6	4986	10	1.87	± 0.59	no
ASTR 1.1.3	2.0	20.0	49.1	20.1	50.1	95636	12.4	4989	10	2.46	± 0.55	no
ASTR 1.1.4	2.0	21.9	45.1	1.9	68.2	95072	9.3	4991	10	1.74	± 0.25	no
ASTR 1.1.5	2.0	22.0	44.9	2.0	67.3	95116	10.6	4993	10	2.06	± 0.45	no
ASTR 1.1.6	2.0	21.9	45.2	2.1	68.2	95101	12.4	4991	10	2.47	± 0.60	no
ASTR 1.1.7	2.0	22.0	45.0	-3.0	65.8	95000	9.3	4989	10	2.04	± 0.45	no
ASTR 1.1.8	2.0	22.0	45.0	-3.0	65.8	95000	10.5	4989	10	2.41	± 0.76	no
ASTR 1.1.9	2.0	21.9	45.2	-3.0	62.9	94992	12.4	4989	10	2.97	± 0.31	no

Table 5: Exhaust Air Transfer Ratio (EATR), Condensation Rotor, without purge sector

EATR without purge sector	v m/s	t_{11} °C	φ_{11} % r.F.	t_{21} °C	φ_{21} % r.F.	p_{Baro} Pa	n rpm	q_{m22} kg/h	Δp_{22-11} Pa	EATR %		Purge Sector
EATR 1.1.1	2.0	20.2	50.1	19.9	50.6	96460	9.3	4993	10	2.18	± 0.14	no
EATR 1.1.2	2.0	20.0	50.1	20.3	49.2	96476	10.6	4993	10	2.51	± 0.14	no
EATR 1.1.3	2.0	19.8	50.5	20.1	49.7	96531	12.4	4993	10	3.05	± 0.17	no
EATR 1.1.4	2.0	21.9	45.2	2.1	67.2	96428	9.3	4993	10	2.24	± 0.14	no
EATR 1.1.5	2.0	21.9	45.1	2.0	68.7	96506	10.6	4993	10	2.51	± 0.17	no
EATR 1.1.6	2.0	22.1	44.4	1.9	69.4	96508	12.4	4993	10	3.07	± 0.18	no
EATR 1.1.7	2.0	21.8	45.5	-3.0	65.1	96391	9.3	4992	10	2.19	± 0.14	no
EATR 1.1.8	2.0	21.9	44.9	-3.2	66.4	96389	10.5	4992	10	2.56	± 0.16	no
EATR 1.1.9	2.0	21.9	45.0	-3.0	68.1	96350	12.4	4992	10	3.12	± 0.17	no

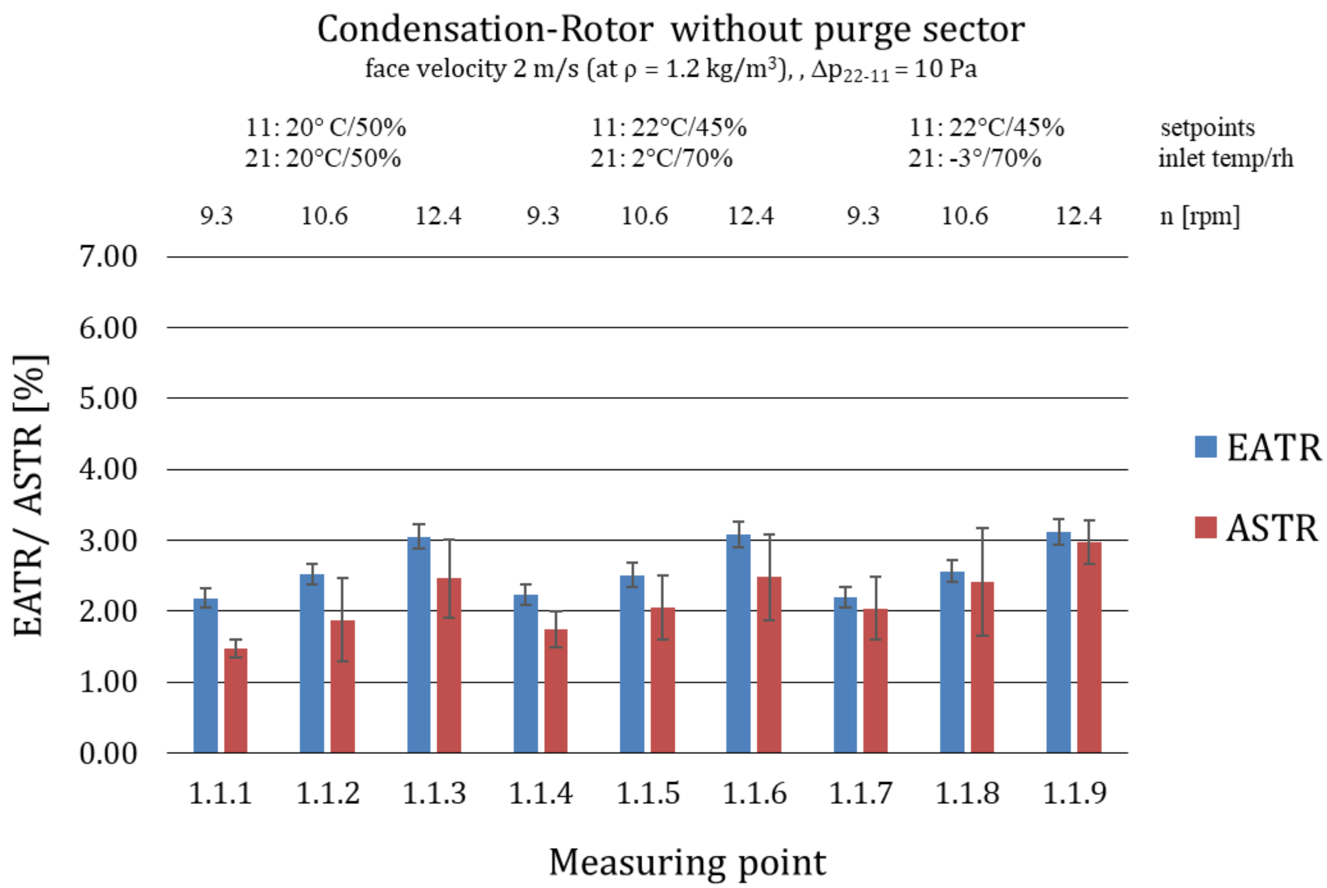

Figure 1: Aerosol Transfer Ratio/ Exhaust Air Transfer Ratio, Condensation Rotor, without purge sector

3.2. Condensation Rotary Heat Exchanger with purge sector

Table 6: Aerosol Transfer Ratio (ASTR), Condensation Rotor, with purge sector

ASTR with purge sector	v m/s	t_{11} °C	φ_{11} % r.F.	t_{21} °C	φ_{21} % r.F.	p_{Baro} Pa	n rpm	q_{m22} kg/h	Δp_{22-11} Pa	ASTR %		Purge Sector
ASTR 1.2.1	2.0	19.9	50.3	20.1	49.1	96339	9.3	4992	10	0.17	± 0.04	yes
ASTR 1.2.2	2.0	19.9	50.7	20.5	48.6	96365	10.6	4993	10	0.26	± 0.06	yes
ASTR 1.2.3	2.0	19.9	50.1	20.0	50.2	96304	12.4	4993	10	0.36	± 0.06	yes
ASTR 1.2.4	2.0	21.8	45.2	2.1	68.0	96074	9.3	4993	11	0.21	± 0.08	yes
ASTR 1.2.5	2.0	22.2	44.5	1.9	67.9	96122	10.6	4994	10	0.31	± 0.05	yes
ASTR 1.2.6	2.0	21.8	45.2	2.0	68.1	96199	12.4	4992	10	0.49	± 0.16	yes
ASTR 1.2.7	2.0	22.0	45.0	-3.1	65.2	95967	9.3	4972	9	0.26	± 0.10	yes
ASTR 1.2.8	2.0	22.2	44.2	-3.0	66.7	95905	10.5	4990	11	0.35	± 0.13	yes
ASTR 1.2.9	2.0	22.0	45.3	-2.8	65.4	95852	12.4	4989	11	0.56	± 0.22	yes

Table 7: Exhaust Air Transfer Ratio (EATR), Condensation Rotor, with purge sector

EATR with purge sector	v m/s	t_{11} °C	φ_{11} % r.F.	t_{21} °C	φ_{21} % r.F.	p_{Baro} Pa	n rpm	q_{m22} kg/h	Δp_{22-11} Pa	EATR %		Purge Sector
EATR 1.2.1	2.0	20.2	50.1	19.9	50.6	96460	9.3	4993	10	0.00	± 0.14	yes
EATR 1.2.2	2.0	20.0	50.1	20.3	49.2	96476	10.6	4993	10	0.03	± 0.13	yes
EATR 1.2.3	2.0	19.8	50.5	20.1	49.7	96531	12.4	4993	10	0.07	± 0.14	yes
EATR 1.2.4	2.0	21.9	45.2	2.1	67.2	96428	9.3	4993	10	-0.02	± 0.14	yes
EATR 1.2.5	2.0	21.9	45.1	2.0	68.7	96506	10.6	4993	10	0.00	± 0.14	yes
EATR 1.2.6	2.0	22.1	44.4	1.9	69.4	96508	12.4	4993	10	0.13	± 0.18	yes
EATR 1.2.7	2.0	21.8	45.5	-3.0	65.1	96391	9.3	4992	10	-0.01	± 0.14	yes
EATR 1.2.8	2.0	21.9	44.9	-3.2	66.4	96389	10.5	4992	10	0.02	± 0.15	yes
EATR 1.2.9	2.0	21.9	45.0	-3.0	68.1	96350	12.4	4992	10	0.11	± 0.14	yes

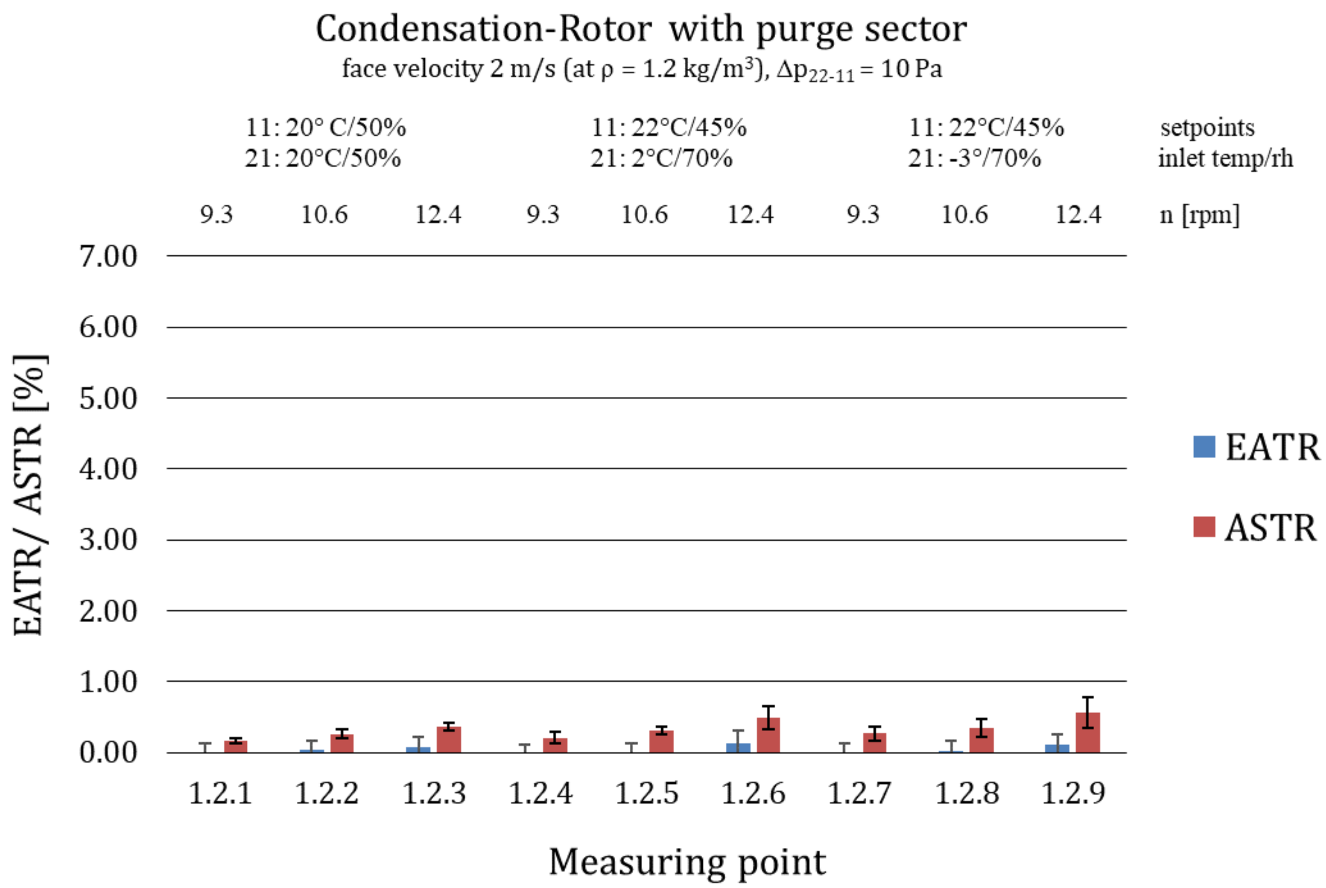

Figure 2: Aerosol Transfer Ratio/ Exhaust Air Transfer Ratio, Condensation Rotor, with purge sector

3.3. Sorption Rotary Heat Exchanger without purge sector

Table 8: Aerosol Transfer Ratio, Sorption Rotor, without purge sector

ASTR without purge sector	v m/s	t_{11} °C	φ_{11} % r.F.	t_{21} °C	φ_{21} % r.F.	p_{Baro} Pa	n rpm	q_{m22} kg/h	Δp_{22-11} Pa	ASTR %		Purge Sector
ASTR 2.1.1	2.0	19.8	51.0	19.9	49.9	94516	10.1	2714	20	1.30	± 0.20	no
ASTR 2.1.2	2.0	20.1	50.0	20.0	50.2	96543	15.1	2714	20	2.51	± 0.29	no
ASTR 2.1.3	2.0	19.9	50.5	20.0	50.2	97631	20.0	2714	20	4.01	± 0.75	no
ASTR 2.1.4	2.0	22.1	44.8	2.1	67.1	97005	10.2	2714	20	1.52	± 0.13	no
ASTR 2.1.5	2.0	22.0	44.8	2.0	67.6	97639	15.1	2714	20	3.14	± 0.77	no
ASTR 2.1.6	2.0	21.8	45.3	2.0	68.7	97665	20.0	2714	20	4.96	± 1.34	no
ASTR 2.1.7	2.0	21.9	45.1	-3.0	65.8	97723	10.3	2714	20	1.83	± 0.21	no
ASTR 2.1.8	2.0	22.0	44.6	-3.1	66.2	97710	15.3	2714	20	3.50	± 0.81	no
ASTR 2.1.9	2.0	22.0	44.9	-3.1	66.5	97690	20.0	2714	20	5.08	± 1.60	no
ASTR 2.1.10	2.0	25.1	45.1	35.1	49.2	97768	10.4	2714	20	0.77	± 0.22	no
ASTR 2.1.11	2.0	25.1	44.6	35.2	49.4	97738	15.2	2714	20	1.43	± 0.42	no
ASTR 2.1.12	2.0	25.1	45.5	35.5	47.8	97745	20.0	2714	20	1.99	± 0.37	no

Table 9: Exhaust Air Transfer Ratio, Sorption Rotor, without purge sector

EATR without purge sector	v m/s	t_{11} °C	φ_{11} % r.F.	t_{21} °C	φ_{21} % r.F.	p_{Baro} Pa	n rpm	q_{m22} kg/h	Δp_{22-11} Pa	EATR %		Purge Sector
EATR 2.1.1	2.0	20.1	49.6	20.0	50.2	97936	10.1	2714	20	2.39	± 0.15	no
EATR 2.1.2	2.0	20.1	49.4	19.9	51.3	98394	15.0	2714	20	4.01	± 0.22	no
EATR 2.1.3	2.0	20.1	49.8	20.1	49.9	98409	20.0	2714	20	5.46	± 0.23	no
EATR 2.1.4	2.0	22.0	44.6	1.9	67.8	98381	10.2	2714	20	2.48	± 0.15	no
EATR 2.1.5	2.0	22.0	44.7	2.1	67.9	98388	15.1	2714	20	4.10	± 0.19	no
EATR 2.1.6	2.0	22.0	44.7	2.0	67.9	98407	20.0	2714	20	5.59	± 0.23	no
EATR 2.1.7	2.0	22.2	44.5	-3.1	68.1	98377	10.3	2714	20	2.53	± 0.15	no
EATR 2.1.8	2.0	22.1	44.8	-3.1	67.3	98397	15.2	2713	20	4.14	± 0.20	no
EATR 2.1.9	2.0	21.9	45.0	-2.9	68.3	98394	20.0	2712	20	5.59	± 0.26	no
EATR 2.1.10	2.0	24.9	44.1	34.9	49.9	97743	10.4	2714	20	2.36	± 0.14	no
EATR 2.1.11	2.0	25.0	43.8	34.9	50.1	97725	15.6	2714	20	3.94	± 0.19	no
EATR 2.1.12	2.0	24.9	44.5	34.9	50.3	97756	20.1	2714	20	5.25	± 0.22	no

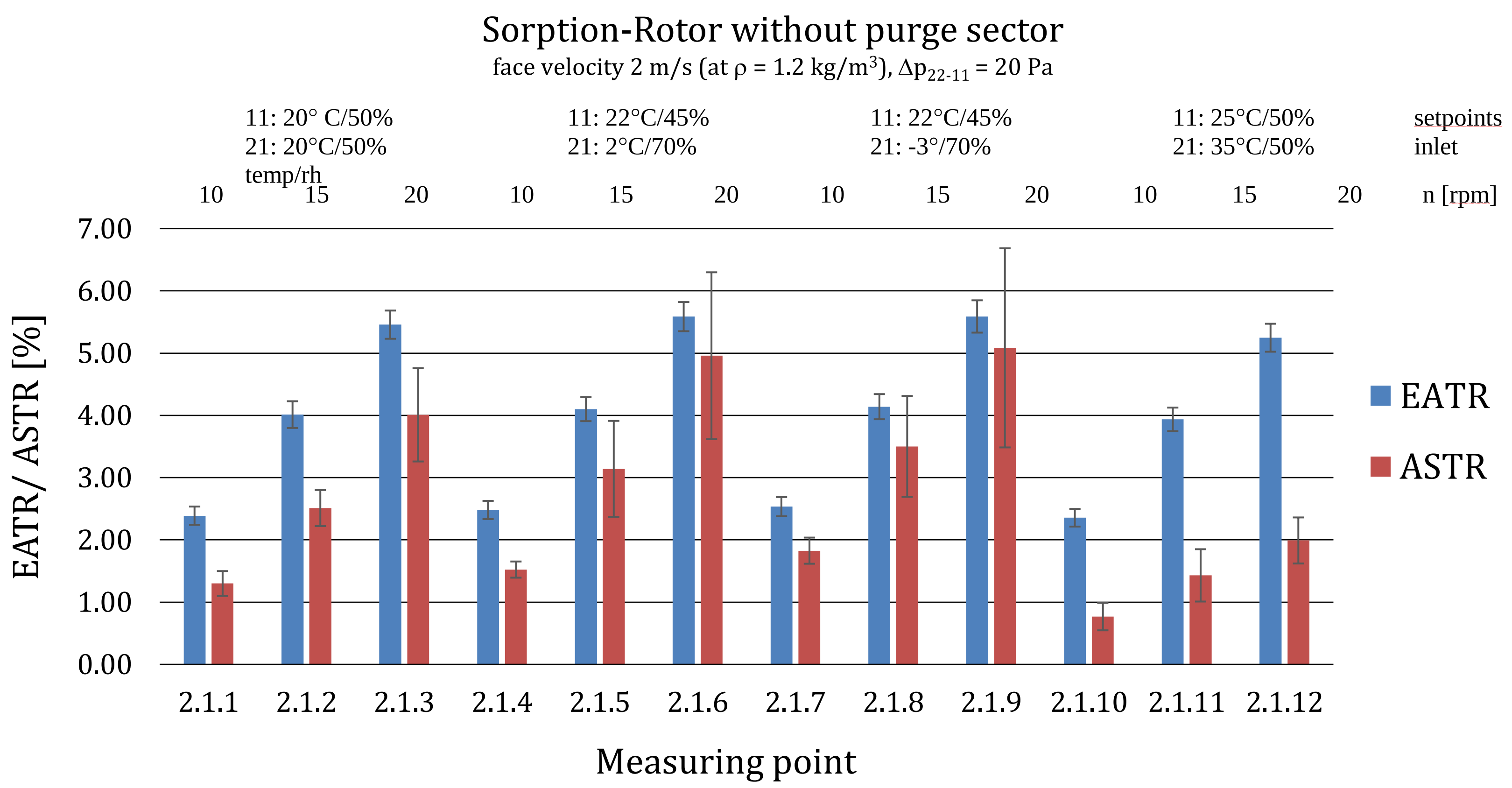

Figure 3: Aerosol Transfer Ratio/ Exhaust Air Transfer Ratio, Sorption Rotor, with purge sector

3.4. Sorption Rotary Heat Exchanger with purge sector

Table 10: Aerosol Transfer Ratio, Sorption Rotor, with purge sector

ASTR with purge sector	v m/s	t_{11} °C	φ_{11} % r.F.	t_{21} °C	φ_{21} % r.F.	p_{Baro} Pa	n rpm	q_{m22} kg/h	Δp_{22-11} Pa	ASTR %		Purge Sector
ASTR 2.2.1	2.0	19.8	51.0	19.9	49.9	94516	10.1	2714	20	0.01	± 0.01	yes
ASTR 2.2.2	2.0	20.1	50.2	20.0	49.7	94540	15.1	2714	20	0.04	± 0.02	yes
ASTR 2.2.3	2.0	20.0	50.3	20.0	49.6	94550	20.0	2714	20	0.18	± 0.07	yes
ASTR 2.2.4	2.0	22.0	45.3	2.0	66.9	94510	10.2	2714	20	0.02	± 0.01	yes
ASTR 2.2.5	2.0	22.1	45.0	2.0	68.0	94493	15.1	2714	20	0.09	± 0.01	yes
ASTR 2.2.6	2.0	22.0	45.4	2.1	66.0	94487	20.0	2714	20	0.34	± 0.07	yes
ASTR 2.2.7	2.0	22.0	45.8	-3.1	66.3	94664	10.3	2713	20	0.02	± 0.01	yes
ASTR 2.2.8	2.0	22.2	44.7	-3.1	67.8	94587	15.3	2714	20	0.12	± 0.03	yes
ASTR 2.2.9	2.0	21.9	45.8	-2.9	62.9	94539	20.0	2714	20	0.40	± 0.14	yes
ASTR 2.2.10	2.0	25.3	49.2	34.9	50.1	95442	10.3	2714	20	0.01	± 0.01	yes
ASTR 2.2.11	2.0	25.1	50.0	35.0	49.4	95409	15.4	2714	20	0.01	± 0.01	yes
ASTR 2.2.12	2.0	24.9	50.4	35.1	49.8	95334	20.1	2714	20	0.06	± 0.04	yes

Table 11: Exhaust Air Transfer Ratio, Sorption Rotor, with purge sector

ETAR with purge sector	v m/s	t_{11} °C	φ_{11} % r.F.	t_{21} °C	φ_{21} % r.F.	p_{Baro} Pa	n rpm	q_{m22} kg/h	Δp_{22-11} Pa	EATR %		Purge Sector
EATR 2.2.1	2.0	20.0	50.1	19.9	50.5	95833	10.1	2714	20	0.00	± 0.15	yes
EATR 2.2.2	2.0	20.0	49.6	20.0	50.3	95846	15.1	2714	20	0.00	± 0.15	yes
EATR 2.2.3	2.0	20.0	50.2	20.0	49.2	95790	20.0	2714	20	0.21	± 0.15	yes
EATR 2.2.4	2.0	22.1	44.6	1.8	67.6	95777	10.1	2714	20	0.00	± 0.16	yes
EATR 2.2.5	2.0	22.2	44.2	2.0	67.8	95759	15.2	2714	20	0.01	± 0.17	yes
EATR 2.2.6	2.0	22.1	44.7	2.0	68.5	95684	20.0	2714	20	0.22	± 0.16	yes
EATR 2.2.7	2.0	21.8	46.0	-3.0	63.9	94811	10.3	2713	20	0.00	± 0.15	yes
EATR 2.2.8	2.0	22.2	45.4	-2.9	62.6	94902	15.3	2713	20	0.00	± 0.15	yes
EATR 2.2.9	2.0	21.8	45.3	-3.0	66.8	95075	20.0	2714	20	0.25	± 0.17	yes
EATR 2.2.10	2.0	25.0	50.0	34.9	50.4	96775	10.4	2714	20	0.00	± 0.14	yes
EATR 2.2.11	2.0	24.9	50.2	35.0	49.7	96897	15.6	2714	20	0.00	± 0.14	yes
EATR 2.2.12	2.0	25.0	50.2	34.8	50.8	97011	20.1	2714	20	0.16	± 0.14	yes

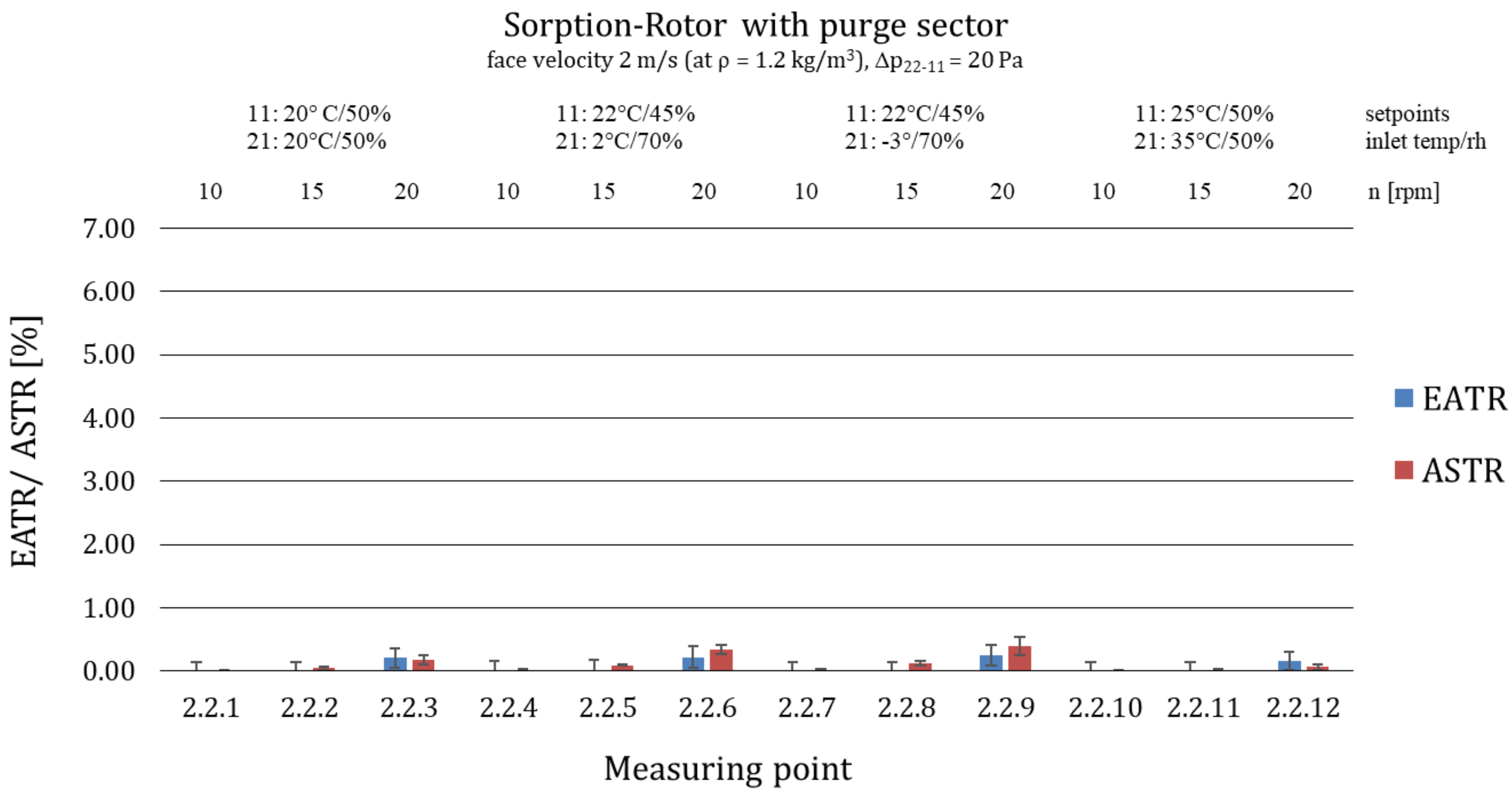

Figure 4: Aerosol Transfer Ratio/ Exhaust Air Transfer Ratio, Sorption Rotor, with purge sector

4. Discussion

4.1. Significance of test conditions

AHUs that comply with the European Ecodesign Regulation [5] are typically designed for a face velocity (related to the inner cross-sectional area of the casing) of about 1.6 to 1.8 m/s at nominal air flow rate. Since the face area of the RHE is usually more than 20% smaller than the cross-sectional area of the AHU, the nominal face velocity of a RHE is usually higher than 2 m/s.
In applications such as office buildings and schools, face velocities in the range of about 1 m/s often occur in partial load operation mode. On the other hand, the REHVA COVID-19 guideline recommends not using partial load operation in pandemic situations. Therefore, the measured EATR and ASTR at 2 m/s are considered conservative for an infection risk assessment.

4.2. Comparison of test results

The following figures summarize the test results from the present project as well as from the previous project [6]. In them, the rotors are designated as follows:

- Condensation Rotor 1: Condensation rotor of the present project, see Table 1.
- Sorption Rotor 1: Sorption rotor of the present project, see Table 1.
- Condensation Rotor 2: Condensation rotor of the previous project
- Sorption Rotor 2: Sorption rotor of the previous project

Condensation Rotor 2 and Sorption Rotor 2 had no purge sector.

Figure 5 shows the ASTR of Condensation Rotor 1 with and without purge sector, as function of the rotor speed by different outdoor air temperatures (according to EN 308: supply air inlet temperature). The face velocity is 2 m/s.

Figure 6 shows the EATR of Condensation Rotor 1 with and without purge sector, as function of the rotor speed by different outdoor air temperatures (according to EN 308: supply air inlet temperature). The face velocity is 2 m/s.

Figure 7 shows the ASTR of Sorption Rotor 1 with and without purge sector, as function of the rotor speed by different outdoor air temperatures (according to EN 308: supply air inlet temperature). The face velocity is 2 m/s.

Figure 8 shows the EATR of Sorption Rotor 1 with and without purge sector, as function of the rotor speed by different outdoor air temperatures (according to EN 308: supply air inlet temperature). The face velocity is 2 m/s.

Figure 9 shows the ASTR and EATR of Condensation Rotor 2 as function face velocity by two different pressure differences $\Delta p_{22\text{-}11}$.

Figure 10 shows ASTR and EATR of Sorption Rotor 2 as function face velocity by two different rotor speeds.

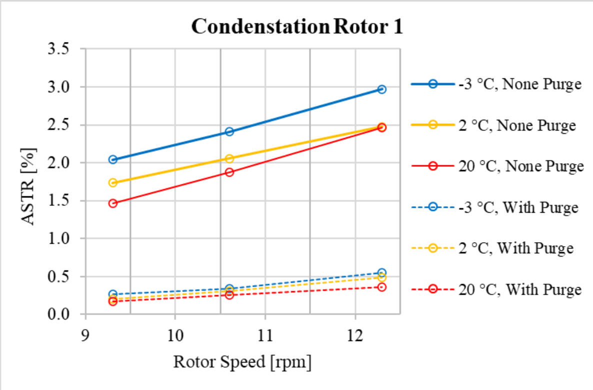

Figure 6: ASTR of Condensation Rotor 1 with and without purge sector, as function of the rotor speed by different outdoor air temperatures and a face velocity of 2 m/s

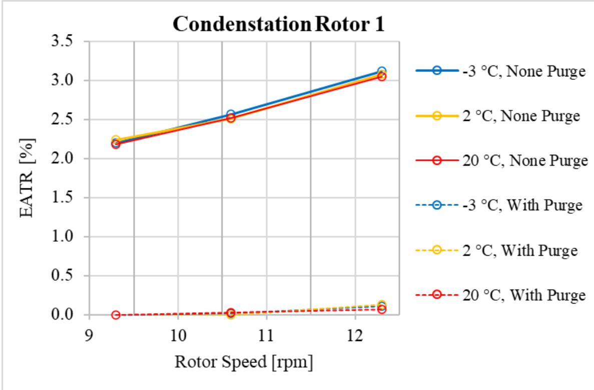

Figure 6: EATR of Condensation Rotor 1 with and without purge sector, as function of the rotor speed by different outdoor air temperatures and a face velocity of 2 m/s

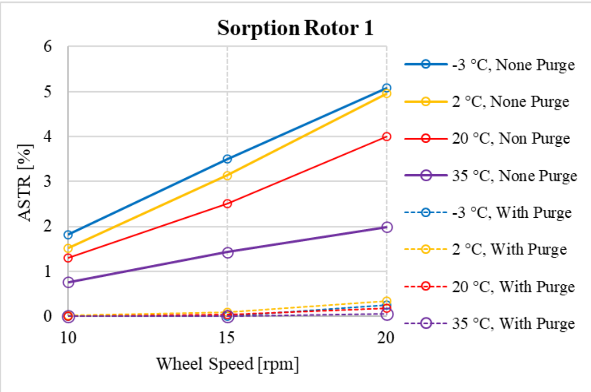

Figure 8: ASTR of Sorption Rotor 1 with and without purge sector, as function of the rotor speed by different outdoor air temperatures and a face velocity of 2 m/s

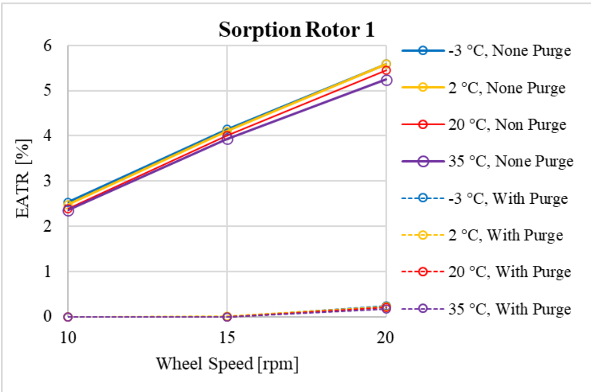

Figure 8: EATR of Sorption Rotor 1 with and without purge sector, as function of the rotor speed by different outdoor air temperatures and a face velocity of 2 m/s

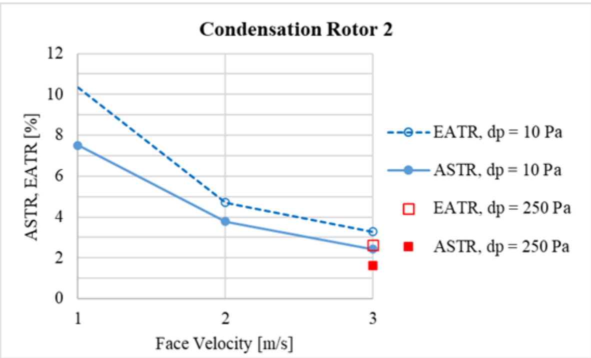

Figure 10: ASTR and EATR of Condensation Rotor 2 as function of the face velocity by two different pressure differences Δ*p*$_{22\text{-}11}$

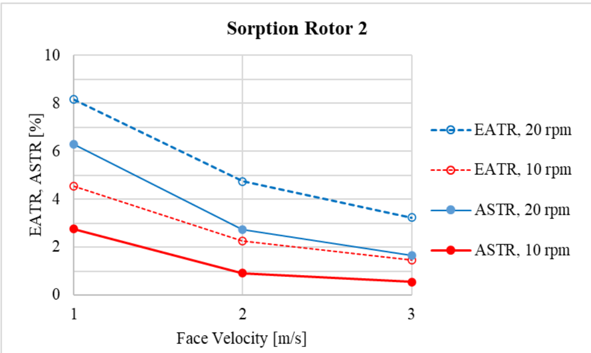

Figure 10: ASTR and EATR of Sorption Rotor 2 as function of the face velocity by two different rotor speeds

Tests without purge sector

At isothermal conditions (20 °C) and a face velocity of 2 m/s in all measurements the ASTR was between 1% and 2% below the EATR.

A clear influence of the temperature can be seen in the ASTR measurements of Condensation Rotor 1 and Sorption Rotor 1. As the outdoor air temperature increases, the ASTR decreases. For the sorption rotor, this tendency is clearer than for the condensation rotor. This temperature-dependence may be partly due to shrinkage of some of the hygroscopic aerosol droplets below the lower detection limit of the sensors with decreasing relative humidity. The observation that the reduction is evident mostly for the sorption rotor would be in support such a mechanism.
The slight tendency for the EATR to be temperature-dependent can be explained by the definition of the face velocity, which is based on standard conditions. Mainly on the outdoor air side, the effective face velocity varies with temperature.

For Condensation Rotor 1 and Sorption Rotor 1, the dependence of EATR and ASTR, respectively, on rotor speed appears to be linear. But the intersection with the abscissa is not at zero, but in the range between 2 and 5 rpm for the ASTR and between 1 and 2 rpm for the ETAR. For the rotors from the previous project there are too few tests for a conclusion about this.

Tests with purge sector
These tests concern only Condensation Rotor 1 and Sorption Rotor 1.

At the low and medium rotor speed, the EATR is practically zero for both rotors (highest measured value 0.03% ± 0.14% [1]). At the highest rotor speed, a maximum EATR of 0.13% ± 0.18% was measured for the condensation rotor and 0.25% ± 0.17% for the sorption rotor. It should be mentioned that, according to the manufacturer, the purge sector of Condensation Rotor 1 is not designed for the maximum rotor speed used in the tests. According to the manufacturer, the purge sector of Sorption Rotor 1 is designed for the highest rotor speed used in the tests.

For Sorption Rotor 1, the ASTR ranges from 0.01% to 0.12% (measurement uncertainty of about 0.02%) at the low and medium rotor speed and 0.40% ± 0.14% at the highest rotor speed.
The ASTR of Condensation Rotor 1 is in the range of 0.17% to 0.35% (with a measurement uncertainty of about 0.10% abs.) at the lower and medium rotor speed and of 0.56% ± 0.22 at the highest rotor speed.

Compared to the tests without purge sector, the measurements with purge sector show an ASTR that is higher than the EATR. For Sorption Rotor 1 with the lower and medium rotor speed, the difference is between 0.01% and 0.12%. For the highest rotor speed, the difference increases slightly to 0.03% to 0.15%. For all rotor speeds, the differences are within the measurement uncertainty, but always in the same direction. For Condensation Rotor 1 with low and medium rotor speed, the difference between ASTR and EATR is between 0.17 % and 0.33 %. At the highest rotor speed, the difference increases slightly to 0.29 % to 0.45 %. For Condensation Rotor 1 differences are greater than the measurement uncertainty.

One difference between the test series of the two rotors was the pressure difference between the supply air outlet and the exhaust air inlet Δp_{22-11}: for the Condensation Rotor 1 it was set to 10 Pa and for the Sorption Rotor 1 to 20 Pa. Since at the lower and medium rotor speed, the EATR of both rotors did not exceed 0.03%, the difference in pressure difference is not sufficient to explain the difference in ASTR. For a more detailed analysis, the fluidic phenomena in the purge sectors would have to be investigated in detail.

It is worth mentioning that even the highest EATR and ASTR values measured at a rotor speed for which the purge sectors are designed can still be considered quite low compared to other leakage and exhaust air transfer risks in ventilation systems.

[1] The value ± 0.14% stands for the absolute measurement uncertainty

4.3. Conclusion

The project investigated how aerosols, which behave similarly to human lung aerosols, are transferred in rotary heat exchangers with and without a purge sector.

For a commercial condensation rotor and a commercial sorption rotor without a purge sector, the aerosol transfer ratio (ASTR) was always lower than the exhaust air transfer ratio (EATR) with the tracer gas SF6. The smallest difference of 0.1 to 0.5 percentage points was found at the lowest tested outside air temperature of -3 °C. At higher outdoor air temperatures, the ASTR was between 0.5 and 2 percentage points lower than the EATR.

With a purge sector and conditions (rotor speed, face velocity, pressure conditions) resulting in an EATR below 0.03%, measurements on a sorption rotor showed a maximum ASTR of 0.12%. For a Condensation rotor with a different purge sector design, the ASTR remained at a level of 0.17 to 0.35%. It is assumed that the difference lies in the fluidic phenomena of the purge sector and not in the matrix of the rotor.

5. List of Figures

Figure 1: Aerosol Transfer Ratio/ Exhaust Air Transfer Ratio, Condensation Rotor, without purge sector 8
Figure 2: Aerosol Transfer Ratio/ Exhaust Air Transfer Ratio, Condensation Rotor, with purge sector. 10
Figure 3: Aerosol Transfer Ratio/ Exhaust Air Transfer Ratio, Sorption Rotor, with purge sector......... 12
Figure 4: Aerosol Transfer Ratio/ Exhaust Air Transfer Ratio, Sorption Rotor, with purge sector......... 14
Figure 5: ASTR of Condensation Rotor 1 with and without purge sector, as function of the rotor speed by different outdoor air temperatures and a face velocity of 2 m/s 16
Figure 6: EATR of Condensation Rotor 1 with and without purge sector, as function of the rotor speed by different outdoor air temperatures and a face velocity of 2 m/s 16
Figure 7: ASTR of Sorption Rotor 1 with and without purge sector, as function of the rotor speed by different outdoor air temperatures and a face velocity of 2 m/s 16
Figure 8: EATR of Sorption Rotor 1 with and without purge sector, as function of the rotor speed by different outdoor air temperatures and a face velocity of 2 m/s 16
Figure 9: ASTR and EATR of Condensation Rotor 2 as function of the face velocity by two different pressure differences $\Delta p_{22\text{-}11}$ 16
Figure 10: ASTR and EATR of Sorption Rotor 2 as function of the face velocity by two different rotor speeds 16
Figure 11: ASTR measurements 20
Figure 12: EATR measurements 21
Figure 13: Heat recovery test rig 22

6. Bibliography

[1] Federation of European Heating, Ventilation and Air Conditioning Associations. RHEVA COVID-19 guidance document, version 4.1. Brussels. 2021-04-15.

[2] EN 308:2021 Heat exchangers - Test procedures for establishing performance of air to air heat recovery components. CEN, Brussels.

[3] Johnsona G.R., Morawskaan L., Ristovskia Z.D., Hargreavesa M., Mengersena K., Chaob C.Y.H., Wanb M.P., Lic Y., Xiecf X., Katoshevskid D., Corbett S. Modality of human expired aerosol size distributions. Journal of Aerosol Science 2011; 42.

[4] Maximoff S.N., Salehi A.A., Rostami A. Modality of human expired aerosol size distributions. Molecular dynamics simulations of homogeneous nucleation of liquid phase in highly supersaturated propylene glycol vapors; 2021

[5] Commission Regulation (EU) No 1253/2014 of 7 July 2014 implementing Directive 2009/125/EC of the European Parliament and of the Council with regard to ecodesign requirements for ventilation units.

[6] Prüfstelle Gebäudetechnik. Test Report No.: HP-202084 Measurements on two Rotary Heat Exchangers. University of Applied Sciences and Arts (HSLU), Horw. 2021-03-09.

7. Annex 2: Test Method

7.1. Aerosol Transfer Ratio ASTR

For the aerosol measurements, a particle generator was installed in the exhaust air inlet duct and additional measuring devices in all four air streams. A mixture of triethylene glycol, monopropylene glycol and dipropylene glycol is used as the aerosol source. The aerosol used has an average diameter of just over one micrometer and is therefore comparable in size to exhaled aerosol. The aerosol, like human exhaled aerosol, is liquid at normal ambient temperatures. It is produced by evaporation and condensation of a water -glycol mixture and is stable in air for extended periods of time.
The aerosol concentration is measured in all four air streams (outside air, supply air, extract air, exhaust air). To keep the aerosol concentration in the outside air as low as possible, it is passed through an H14 filter. In the exhaust air inlet, the aerosol feed is built up. During the measurement, the aerosol is applied using a pulse method. The maximum peak heights at the four aerosol measuring points are used for evaluation. Parallel to the aerosol transfer, the EATR is determined with tracer gas.

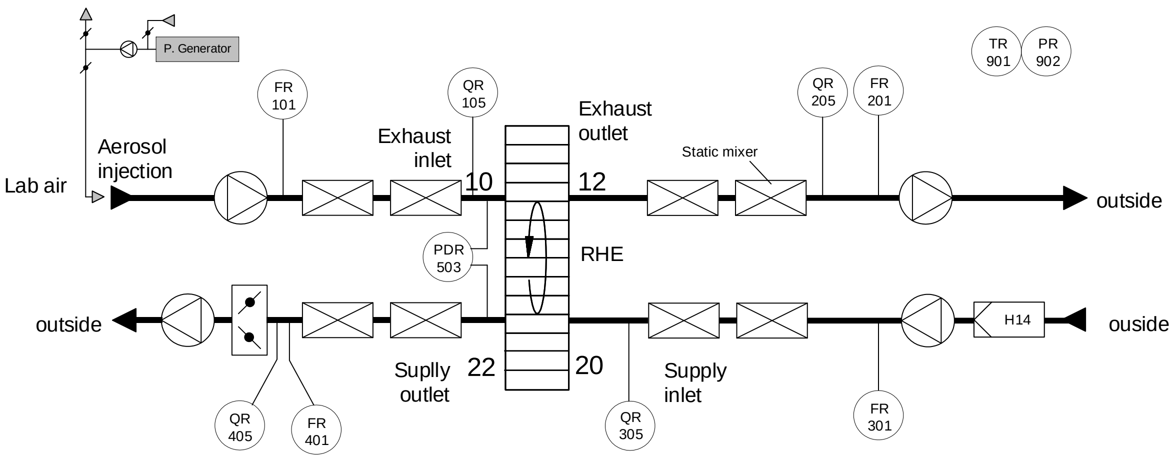

Figure 11: ASTR measurements

Table 12: Symbols ASTR measurements

First letter	Subsequent letter	Auxiliary letter
F air flow rate P pressure T temperature M humidity Q concentration	D difference	R registration

Table 13: Measured values ASTR tests

Position	Symbol	Unit	Description
FR101	q_{v11}	m^3/h	Volume flow extract air 1.1
QR105	b_{11}	P/cm^3	Aerosol concentration extract air 1.1
QR205	b_{12}	P/cm^3	Aerosol concentration exhaust air 1.2
QR305	b_{21}	P/cm^3	Aerosol concentration outdoor air 2.1
FR401	q_{v22}	m^3/h	Volume flow supply air 2.2
QR405	b_{22}	P/cm^3	Aerosol concentration supply air 2.2
TR901	t_u	°C	Ambient temperature
PR902	p_{baro}	Pa	Atmospheric pressure

Table 14: Calculated values ASTR tests

Symbol	Unit	Description	Definition
ASTR	%	Aerosol transfer ratio	$ASTR = \frac{q_{ASTR}}{q_{m22}} \cdot 100\% = \frac{b_{22} - b_{21}}{b_{11} - b_{21}} \cdot 100\%$

7.2. Exhaust Air Transfer Ratio EATR

Measurement for EATR is conducted by injecting SF_6 Sulphur Hexafluorid Tracergas in the Extract Air (1.1) of the heat recovery test rig. SF_6 concentration is determined with a photoacoustic IR-gas monitor in all four stations.

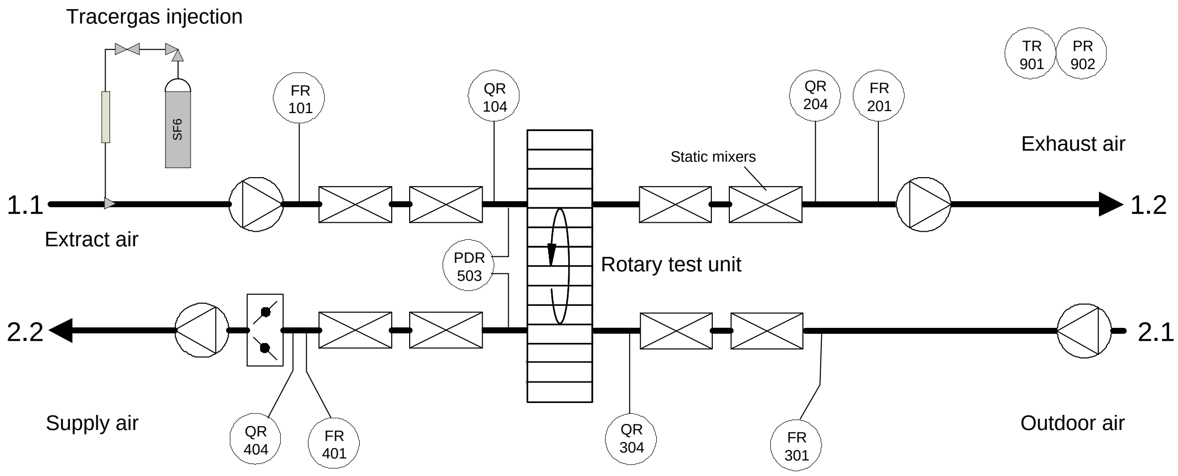

Figure 12: EATR measurements

Table 15: Symbols EATR measurements

First letter	Subsequent letter	Auxiliary letter
F air flow rate P pressure T temperature M humidity Q concentration	D difference	R registration

Table 16: Measured values EATR tests

Position	Symbol	Unit	Description
FR101	q_{v11}	m^3/h	Volume flow extract air 1.1
QR104	a_{11}	ppm	Tracergas concentration extract air 1.1
QR204	a_{12}	ppm	Tracergas concentration exhaust air 1.2
QR304	a_{21}	ppm	Tracergas concentration outdoor air 2.1
FR401	q_{v22}	m^3/h	Volume flow supply air 2.2
QR404	a_{22}	ppm	Tracergas Concentration supply air 2.2
TR901	t_u	°C	Ambient temperature
PR902	p_{baro}	Pa	Atmospheric pressure

Table 17: Calculated values EATR tests

Symbol	Unit	Description	Definition
EATR	%	Exhaust air transfer ratio	$EATR = \frac{q_{EATR}}{q_{m22}} \cdot 100\% = \frac{a_{22} - a_{21}}{a_{11} - a_{21}} \cdot 100\%$

7.3. Test Rig for Energy Recovery Devices

The standard measurement values as air flow, temperature, humidity, pressure difference are shown in the following figure.

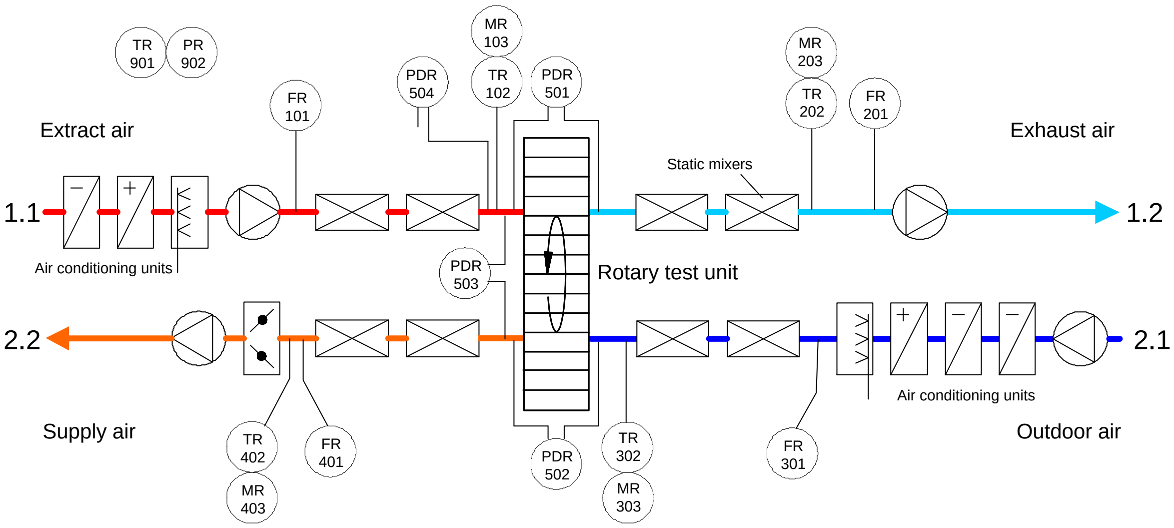

Figure 13: Heat recovery test rig

Table 18: Measured values test rig for energy recovery devices

Position	Symbol	Unit	Description
FR101	q_{v11}	m^3/h	Volume flow extract air 1.1
TR102	t_{11}	°C	Temperature extract air 1.1
MR103	tp_{11}	°C	Dew point temperature extract air 1.1
FR201	q_{v12}	m^3/h	Volume flow exhaust air 1.2
TR202	t_{12}	°C	Temperature exhaust air 1.2
MR203	tp_{12}	°C	Dew point temperature exhaust air 1.2
FR301	q_{v21}	m^3/h	Volume flow outdoor air 2.1
TR302	t_{21}	°C	Temperature outdoor air 2.1
MR303	tp_{21}	°C	Dew point temperature outdoor air 2.1
FR401	q_{v22}	m^3/h	Volume flow supply air 2.2
TR402	t_{22}	°C	Temperature supply air 2.2
MR403	tp_{22}	°C	Dew point temperature supply air 2.2
PDR501	pv_1	Pa	Pressure drop extract air 1.1 – Exhaust air 1.2
PDR502	pv_2	Pa	Pressure drop outdoor air 2.1 – Supply air 2.2
PDR503	Δp_{22-11}	Pa	Pressure difference Supply air 2.2 – Extract air 1.1
PDR504	$\Delta p_{11-baro}$	Pa	Pressure difference Exract air 1.1 – Atmospheric pressure
TR901	t_u	°C	Ambient temperature
PR902	p_{baro}	Pa	Atmospheric pressure

Table 19: Calculated values

Symbol	Unit	Description	Definition
v	m/s	Face air velocity	$v = \frac{q_{vn}}{\frac{A_{tot}}{2}}$
A_{tot}	m^2	Free face area	$A_{tot} = \pi \frac{D_O^2 - D_i^2}{4}$
q_m	kg/s	Air mass flow rate	$q_m = q_{v,meas} \cdot \rho$
ρ	kg/ m^3	Air density measured	$\rho = f(p_{Baro}, t, x)$
x	g/kg	Moisture content	$x = f(p_{Baro}, t, tp)$

7.4. Symbols and Subscripts

1	exhaust-air side
2	supply-air side
11	extract air
12	exhaust air
21	outdoor air
22	supply air
n	rotor speed
ASTR	aerosol transfer ratio
EATR	exhaust air transfer ratio
q_{EATR}	mass flow exhaust air transfer ratio
q_m	air mass flow rate
A_{tot}	free face area
D_O	free diameter

8. Annex 2: Measurement Devices

8.1. Aerosol Generator/ Aerosol

The Aerosol Generator is a *Look Power-Tiny Accu-Power Fogger* fog machine. At full power, the generator produces up to 5*10^13 #/min in the detectable size range (or around 100'000 #/cm^3 in a volume flow of 500 m^3/min).

The aerosol used has an average diameter of just over one micrometer and is therefore comparable in size to exhaled aerosol [2]. The aerosol, like human exhaled aerosol, is liquid at normal ambient temperatures. It is produced by evaporation and condensation of a water-glycol mixture and is stable in air for a long time [3]. The mixture used in the studies consists of triethylene glycol, monopropylene glycol and dipropylene glycol.

8.2. Aerosol measuring device

Two measuring devices were installed in each air duct.

Make: Sensirion
Type: SPS30
Measuring range (number in PM10):
- Size range 0.3 to 10 µm
- calibrated measuring range 0 to 3000 #/cm3, extrapolated linear range up to 100'000 #/cm3. (factory calibration)

Measurement uncertainty ex works for PM4 and PM10: 0-1000 #/cm3 +/-250 #/cm3; > 1000 #/cm3: +/- 25% (determined with Arizona test dust / salt dust by manufacturer)
Measurement uncertainty ex works for PM2.5 and smaller: 0-1000 #/cm3 +/-100 #/cm3; > 1000 #/cm3: +/- 10% (determined with Arizona test dust / salt dust by manufacturer)

Uncertainty* after internal cross correction for number PM10: 0-1000 #/cm3 +/- 10 #/cm3, >1000 #/cm3: +/- 3% (determined with TinyPower test dust in SCOEH test room)

*) Device to Device variability.

8.3. Specification Instruments test rig for energy recovery devices

If there are references to calibration documents the measurement uncertainties are given with a level of confidence of 95% (k=2).

Position	Sensor Number	Symbol	Unit	Measurement Uncertainty	Date of Calibration	Indication	Remarks
PDR 600	1.07 HP 177	p_{wi11}	Pa	2.07 Pa	20.03.2019	Differential Pressure Extract Air 11	
PDR 601	1.07 HP 186	p_{wi12}	Pa	1.84 Pa	20.03.2019	Differential Pressure Exhaust Air 12	
PDR 602	1.07 HP 189	p_{wi21}	Pa	1.42 Pa	20.03.2019	Differential Pressure Outdoor Air 21	
PDR 603	1.07 HP 181	p_{wi22}	Pa	2.61 Pa	20.03.2019	Differential Pressure Supply Air 22	
PDR 505	1.07 HP 154	p_{vor11}	Pa	1.11 Pa	20.03.2019	Pressure Extract Air 11	
PDR 506	1.07 HP 087	p_{vor12}	Pa	2.04 Pa	20.03.2019	Pressure Exhaust Air 12	
PDR 507	1.07 HP 117	p_{vor21}	Pa	1.33 Pa	20.03.2019	Pressure Outdoor Air 21	
PDR 508	1.07 HP 084	p_{vor22}	Pa	1.58 Pa	20.03.2019	Pressure Supply Air 22	
TR 102	1.16 HP 164	t_{11}	°C	0.18 K	01.10.2020	Temperature Extract Air 11	Grid with 16 PT100
TR 202	1.16 HP 164	t_{12}	°C	0.08 K	01.10.2020	Temperature Exhaust Air 12	Grid with 16 PT100
TR 302	1.16 HP 164	t_{21}	°C	0.08 K	01.10.2020	Temperature Outdoor Air 21	Grid with 16 PT100
TR 402	1.16 HP 164	t_{22}	°C	0.10 K	01.10.2020	Temperature Supply Air 22	Grid with 16 PT100
MR 103	1.09 HP 116	tp_{11}	°C	012 K	27.08.2021	Dew Point Extract Air 11	
MR 203	1.09 HP 114	tp_{12}	°C	0.11 K	27.08.2021	Dew Point Exhaust Air 12	
MR 303	1.09 HP 113	tp_{21}	°C	0.13 K	27.08.2021	Dew Point Outdoor Air 21	
MR 403	1.09 HP 115	tp_{22}	°C	0.15 K	27.08.2021	Dew Point Supply Air 22	
PDR 501	1.07 HP 138	Dp_{1}	Pa	0.86 Pa	20.03.2019	Pressure Loss Exhaust Side 1	
PDR 502	1.07 HP 156	Dp_{2}	Pa	0.34 Pa	20.03.2019	Pressure Loss Supply Side 2	
PDR 503	1.07 HP 135	$Dp_{22-11,22-12}$	Pa	3.37 Pa	20.03.2019	Pressure Difference 22-11, 22-21	
PDR 504	1.07 HP 019	Dp_{11-Umg}	Pa	2.56 Pa	20.03.2019	Pressure Difference 22-Umg	

Position	Sensor Number	Symbol	Unit	Measurement Uncertainty	Date of Calibration	Indication	Remarks
TR 901	1.03 HP 126	t_{umg}	°C			Ambient Temperature	not calibrated
PR 902	1.07 HP 202	p_{baro}	mbar	46 Pa	26.03.2019	Barometric Pressure	
	1.11 HP 060					Multipoint Sampler for Tracegas concentration	
	1.11 HP 059	a_{11}, a_{12}, a_{21}, a_{22}	ppm	0.02 ppm + 1.4 % MW	02.08.2020	Concentrations Tracergas 11, 12, 21, 22	
FR 101	1.08 HP 340	-	m3/h	0.77 % MW	14.09.2018	Volumetric Airflow Nozzle DN250 Extract Air 11	
FR 201	1.08 HP 342	-	m3/h	0.76 % MW	14.09.2018	Volumetric Airflow Nozzle DN250 Exhaust Air 12	
FR 301	1.08 HP 343	-	m3/h	0.84 % MW	13.09.2018	Volumetric Airflow Nozzle DN250 Outdoor Air 21	
FR 401	1.08 HP 341	-	m3/h	0.79 % MW	14.09.2018	Volumetric Airflow Nozzle DN250 Supply Air 22	
FR 101	1.08 HP 327	-	m3/h	0.72 % MW	15.09.2018	Volumetric Airflow Nozzle DN150 Extract Air 11	
FR 201	1.08 HP 328	-	m3/h	0.73 % MW	14.09.2018	Volumetric Airflow Nozzle DN150 Exhaust Air 12	
FR 301	1.08 HP 329	-	m3/h	0.71 % MW	14.09.2018	Volumetric Airflow Nozzle DN150 Outdoor Air 21	
FR 401	1.08 HP 326	-	m3/h	0.75 % MW	14.09.2018	Volumetric Airflow Nozzle DN150 Supply Air 22	

Table 20: Specification of Instruments

The measurement uncertainties for temperature, volumetric airflow and pressure drop are within the tolerances of EN 308. They are determined according to the ISO/IEC Standard Guide 98-3:2008 „Guide to the Expression of Uncertainty in Measurements (GUM) “.